International Journal of Power Electronics and Drive System (IJPEDS)
Vol. 17, No. 4, December 2026, pp. 2965~2984
ISSN: 2088-8694, DOI: 10.11591/ijpeds.v17.i4.pp2965-2984

Integrated PV-driven DC–DC converter with hybrid energy storage system for electric vehicle applications

M. Vaigundamoorthi[1], G. Jegadeeswari[1], S. Asha[2], Savitha Venkatesan[1], R. Sundar[3], S. P. Manikandan[2], P. Veera Manikandan[4], Malathy Batumalay[5]
[1]Department of Electrical and Electronics Engineering, Saveetha Engineering College, Chennai, India
[2]Departmentof Electronics and Communication Engineering, Saveetha Engineering College, Chennai, India
[3]Department of Marine Engineering, AMET Deemed to be University, Chennai, India
[4]Department of Electrical and Electronics Engineering, Dhanalakshmi Srinivasan College of Engineering and Technology, Chennai, India
[5]Centre for Data Science and Sustainable Technologies, Faculty of Data Science and Information Technology, INTI International University, Nilai, Malaysia

Article Info

Article history:

Received Feb 21, 2026
Revised Sep 9, 2026
Accepted Sep 17, 2026

Keywords:

Bidirectional converter
Electric vehicles
Hybrid energy storage system
Interleaved KY converter
PV system
SEPIC converter
Vehicle-to-grid

ABSTRACT

This work introduces a power conversion architecture for grid-connected electric vehicle (EV) applications using a photovoltaic (PV) power generation system, a single-ended primary-inductor converter (SEPIC) DC-DC converter, an interleaved KY converter, and a hybrid energy storage system. The SEPIC converter is connected to the PV array; the output voltage is controlled by varying the PV array input voltage under different conditions of solar insolation, and a constant DC-link voltage is achieved. The interleaved KY converter offers high voltage gain, low output-current ripple, high dynamic response, and high conversion efficiency. A cascaded fuzzy logic controller (CFLC) is designed to control the operation of the converter by using an outer voltage-control loop to generate the reference current and an inner current-control loop to calculate the optimal duty ratio for interleaved phases. The hybrid energy storage system is comprised of a battery and supercapacitor to assist EV charging, regenerative braking, as well as peak-power demands, while minimizing the stress on the battery. Moreover, a bidirectional DC-DC converter provides the possibility for vehicle-to-grid (V2G) and controlled bidirectional power transfer between the EV and the utility grid. The effectiveness of voltage regulation, power-flow management, stress on storage elements, and stable charging and discharging operation is confirmed by MATLAB/Simulink results. The proposed architecture is flexible for applications related to renewable energy integration and EV charging and grid interaction.

This is an open access article under the CC BY-SA license.

Corresponding Author:

G. Jegadeeswari
Department of Electrical and Electronics Engineering, Saveetha Engineering College
Chennai, India
Email: Jegadeeswari.dharan@gmail.com

1. INTRODUCTION

The worldwide trend toward sustainable transportation has driven the growth of electric vehicles (EVs), have been inspired by an objective to improve energy efficiency, reduce emissions, and support Sustainable Development Goals (SDG) [1], [2]. However, the rising EV penetration presents a substantial limit to power system stability, load control, and charging infrastructure, especially when the number of EVs charging increases during peak periods [3]. Incorporating green energy sources, particularly photovoltaic (PV) systems, into EV charging networks has emerged as an effective option for reducing operational costs,

decreasing grid stress, and increasing energy independence [4]. PV systems, while economically useful, suffer from intermittent output and nonlinear I–V characteristics, requiring stable power conditioning and modern maximum power point tracking (MPPT) techniques to deliver optimal power extraction [5], [6]. Single-ended primary-inductor converter (SEPIC) converters are generally suggested for PV systems because of their capability to offer wide-range voltage control and maintain a continuous input current [7], [8], making them ideal for connecting PV with other DC converters.

To improve MPPT precision under different load conditions, intelligent algorithms such as ANFIS controllers have been found to provide greater stability and convergence speed compared to traditional techniques [9], [10]. In the case of EV charging, obtaining low ripple and high voltage gain is important, as EV traction batteries need regulated DC power. Conventional boost converters commonly suffer from poor dynamic response and switching losses, while interleaved and KY-based converters deliver improved efficiency, power density, and current-sharing capabilities owing to reduced ripple and phase-shifted operation [11]-[13]. Recent research has emphasized the merits of interleaved KY converters in green energy-powered EV systems, providing an efficient transient response and decreased electromagnetic interference [14], [15]. To improve the stability of the converter, fuzzy logic controllers have been widely employed in nonlinear power electronic systems for handling unpredictability, dynamic loads, and parameter-varying conditions [16], [17].

Hybrid energy storage systems (HESS), which include batteries and supercapacitors, are gaining popularity because of their unique properties and their high energy density. While supercapacitors offer quick charge and discharge capacity, enhancing the lifetime of the system, acceleration, performance during peak loads, and regenerative events [18]-[20]. Additionally, vehicle-to-grid (V2G) methods offer EVs to serve as distributed energy storage units, delivering grid support services including renewable balancing, peak shaving, and reactive power compensation [21], [22]. When integrating with intelligent control and energy control systems, V2G have been shown in these studies to enhance the reliability of the grid and improved power quality problems [23]-[25].

- Problem Statement

The increasing growth in electric vehicles, integrated with the increasing utilization of renewable energy sources, is creating substantial difficulties in offering efficient, stable, and accurate power conversion for grid support and EV charging. Traditional charging systems suffer from various limitations, including inefficient voltage control, variable PV voltage, excessive ripple, delayed dynamic response, and poor integration of hybrid storage systems. Furthermore, existing EV converters frequently lack intelligent control methods capable of controlling varying load and grid conditions, whereas V2G operation requires modern bidirectional energy control. Therefore, there is a need for an efficient power conversion system that can:

i) Effectively boost power from PV under different load conditions.
ii) Regulate and optimize DC voltage for charging EVs by utilizing low-ripple and high-gain converters.
iii) Ensure smooth transfer of power flow between PV, hybrid storage systems, and the grid.
iv) Maintain steady-state operation via advanced control algorithms.

This study discusses these problems by designing a combined PV–SEPIC–interleaved KY converter design incorporated with CFLC to attain efficient voltage control, enhanced dynamic response, and stable bidirectional power flow for modern EV and smart-grid applications. Particularly, the work aims to achieve the following objectives:

i) Design and implement a SEPIC converter with an ANFIS-based MPPT controller to optimize PV power and manage the PV output under different environmental scenarios.
ii) Develop a high-gain EV converter with an interleaved KY converter to attain efficient voltage gain, minimized ripple, and enhanced dynamic performance for EV charging.
iii) Implement a cascaded fuzzy logic controller (CFLC) to enhance the stability of the converter, transient response, and accurate voltage regulation during dynamic load.
iv) To enable bidirectional power flow for vehicle-to-grid functionality through the design of a bidirectional DC–DC converter, facilitating controlled energy exchange between the EV and utility grid.
v) To interface the hybrid system with the grid using a three-phase VSI for seamless integration, stable power injection, and support for home loads and grid balancing.
vi) To simulate the complete PV–SEPIC–interleaved KY-converter system in MATLAB/Simulink and analyze its performance in terms of voltage regulation, converter efficiency, dynamic response, and overall management of energy.

This is the way; the paper is ordered as follows: i) Section 2 covers a detailed methodology, a specification, a thorough explanation of the design parameters, and calculations of output parameters; ii) The analysis of the proposed converters is described in section 3; iii) Results and discussion are presented in section 4; iv) Comparative analysis and the efficacy of the proposed converter are given in section 5; and v) Finally, section 6 provides the conclusion and future work.

2. METHOD

Figure 1 illustrates a fully integrated PV–grid–EV energy ecosystem where power can flow intelligently between solar panels, the home, the electric vehicle, and the utility grid. Solar energy generated by the PV array is processed through a PV converter and fed into the power conditioning system (PCS), which coordinates energy distribution. The PCS includes both a grid converter and an EV battery (EVB) converter, enabling the system to supply power to home loads, charge the EV battery, or inject energy into the grid. Using bidirectional power flow capabilities, the EV battery can also discharge energy back to the home or grid through standards such as CHAdeMO, supporting V2G operation.

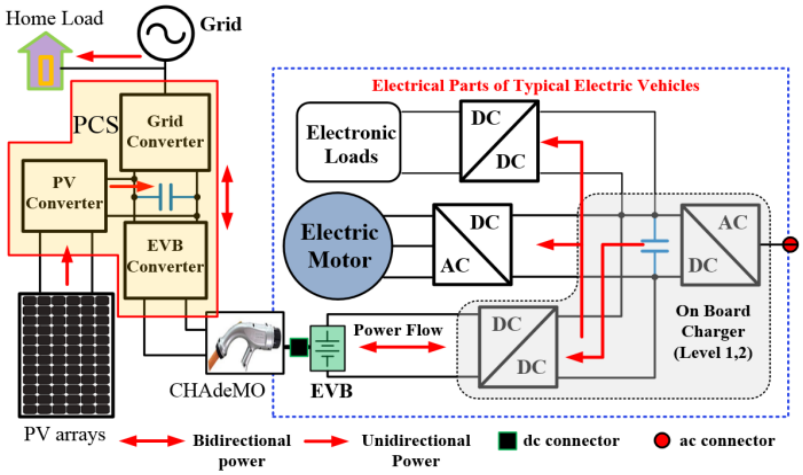

Figure 1. Charging system configuration for an electric vehicle

The internal electrical design of a typical EV is shown on the right side of the configuration, which includes DC-DC converters for auxiliary loads, an on-board charger for AC charging, and DC-AC converters for motor driving. The system illustrates both bidirectional and unidirectional power paths, indicating how energy flows during propulsion, charging, discharging, and grid support. In general, the system shows a modern smart-grid model in which solar power, EV batteries, and the grid are integrated to increase efficiency, improve fast charging, support the stability of the grid, and enhance energy control at both the vehicle and home load.

The PV converter and the solar panels for generating power are illustrated on the left side of the configuration. To get a stable output from the panels, a SEPIC converter is used, which regulates and boosts the varying voltage from the PV panels and offers a constant voltage for charging. The EV converter, placed in the middle part, controls energy exchange with the battery of EVs. It employs either a boost, an interleaved boost, or an interleaved KY converter, depending on the required efficiency and voltage gain. These converters provide optimal charging of the EV battery and also enable bidirectional power flow for V2G operation. On the right, the grid converter connects the PCS to the utility grid through a bidirectional full-bridge converter, providing both V2G and G2V charging and energy return. These system configuration show how the PCS integrates solar power, EV charging, and integration of grid to provide a reliable, flexible and efficient energy control systems.

As can be seen in Figure 2, the power conversion system (PCS) functions as the main unit managing the energy of the renewable energy-based EV charging and grid-interaction system. It manages power flow between the PV converter, EV converter, and grid converter. The PV converter to regulate the PV power is a SEPIC converter; the EV converter to charge the EV is a boost/interleaved boost/interleaved buck converter. The grid converter features a bi-directional DC-DC converter for controlled bi-directional power exchange between the EV and the grid, both for charging and V2G. Therefore, the PCS offers simultaneous power conversion, voltage regulation, and bi-directional energy management between the PV source, the EV, and the power grid.

Figure 3 presents the proposed system, which integrates the combination of renewable energy, a high-gain converter, intelligent control, and a hybrid storage system to provide a highly effective power conversion design for EV applications. Solar energy from the PV array is first processed by the SEPIC converter, which maintains and adjusts the output from the PV under changing irradiance. Maximum power tracking is ensured by an ANFIS-based controller powering the SEPIC through a PWM generator with an

optimal duty ratio. The controlled DC output is then improved by an interleaved KY converter, which is more stable, has the highest voltage gain, and has an enhanced dynamic response. The stable output is further improved by a CFLC by comparing the actual and reference voltages and producing reliable switching pulses. A hybrid system containing a battery and supercapacitor enables fast charging, regenerative braking, and peak power demands while enhancing overall reliability. A bidirectional DC–DC converter permits G2V and V2G power transfer, while a three-phase VSI enables a smooth integration between the grid and home loads. In general, the system offers efficient energy control, stable voltage gain, and improved grid support for future EV and smart-grid applications.

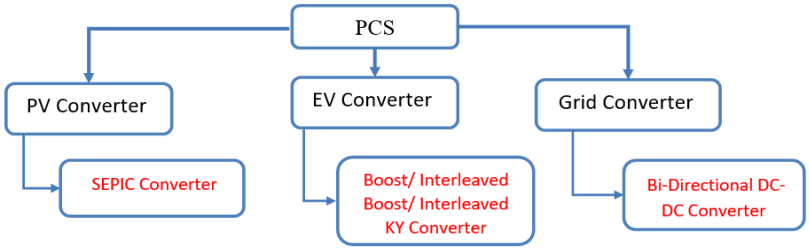

Figure 2. Proposed component system

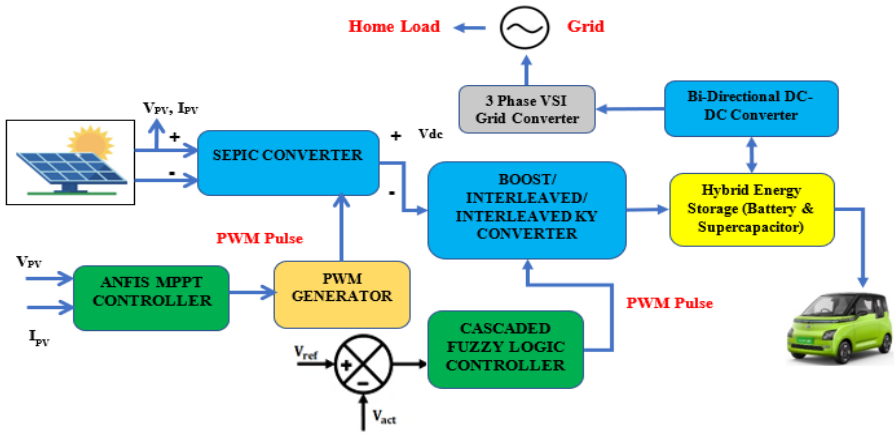

Figure 3. Proposed block diagram

3. ANALYSIS OF PROPOSED CONVERTER

This section presents a detailed analysis of the proposed converter and is depicted in Figure 4. The specifications of the interleaved KY converter are presented in Table 1. Specifications of solar panels and SEPIC converter ratings are given in Table 2, and the calculated values of components for the selected bidirectional DC converter are given in Table 3.

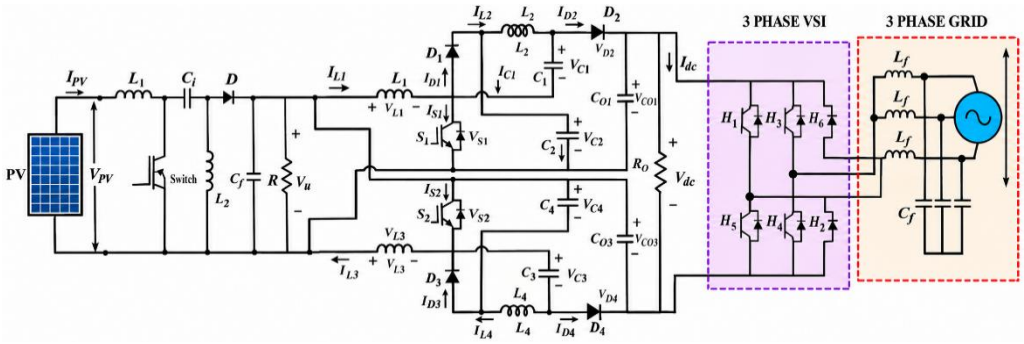

Figure 4. Proposed converter

Table 1. Specifications of IKY

Parameters	Values
Device used	Trans IGBT Module N-CH 1200 V, 400 A, 7-pin Case D-55
Switching frequency	10 KHz
Diode	MCD95
Capacitors C1, C2, C3 and C4	75 µF
Inductor L1, L2, L3 and L4	0.288 mH
Capacitor C01 and C02	150 µF

Table 2. Specifications of solar panel and SEPIC

Parameters		Ratings
Solar panel's	Input voltage	16.8 V
	No. of series cells	38
	Max. voltage	1000 V
	No. of panels	12
	Temperature range	-40 to + 75 ℃
	Input current	5.9 A
SEPIC converter	Diodes	MCD95
	$L1$, $L2$,	0.576 mH
	$C1$, $C2$,	22 µF
	Switching frequency	10 KHZ

Table 3. Calculated values of components used in BDC

Parameters	Values
Duty ratio	0.55
Switching frequency	25 kHz
Output power	24 W
Battery voltage	24 V
Inductor	2.4 mH
Inductor ripple current	0.2 A
Input and output capacitor	4.16 μ F and 41.66 μF
Ripple in capacitor voltage	5%
Battery type	Lithium Ion

3.1. SEPIC converter

The SEPIC is a versatile DC-DC converter that can step-up, step-down, or maintain the output voltage with respect to the input voltage without changing the polarity of the output voltage with respect to the input voltage. The switching duty cycle is the main factor in determining the output voltage and power. The SEPIC converter is made up of two inductors (L1 and L2), an energy transfer capacitor (C1), a diode, a power switch, and an output capacitor (C0). During switching, the energy is transferred from the input source to the load via the coupling capacitor and inductor. The SEPIC topology allows for a very large input voltage range and allows step-up and step-down voltage conversion without any polarity inversion, unlike conventional boost converters. The circuit configuration of the SEPIC converter is given in Figure 5, and the current waveform of the SEPIC converter is shown in Figure 6.

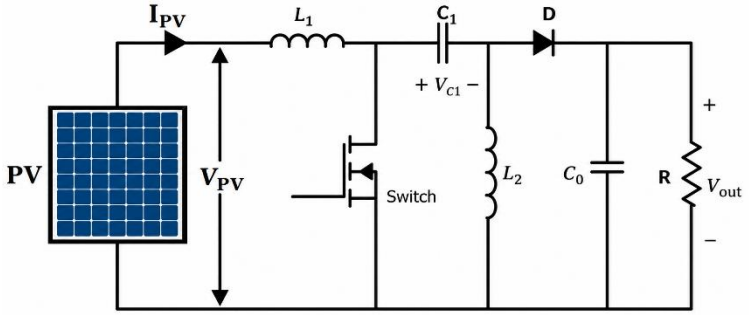

Figure 5. SEPIC converter circuit topology

The voltage gain of the SEPIC converter can be programmed over a wide range by adjusting the duty cycle of the switching, allowing its use in systems having large variations in the input voltage. The voltage stresses on the semiconductor devices are affected by the composite voltage of the input source and the coupling capacitor in switching operation. The proposed design is a SEPIC converter which is designed to get the input voltage as 140 V and the output voltage as 450 V; hence, the proposed design is capable of giving the output voltage that is required. The duty ratio and dependent components in the circuit have an important effect on how SEPIC converters step up or down the voltage. The output voltage of an ideal SEPIC converter is given by (1).

$$V_0 = \frac{D*V_i}{1-D} \quad (1)$$

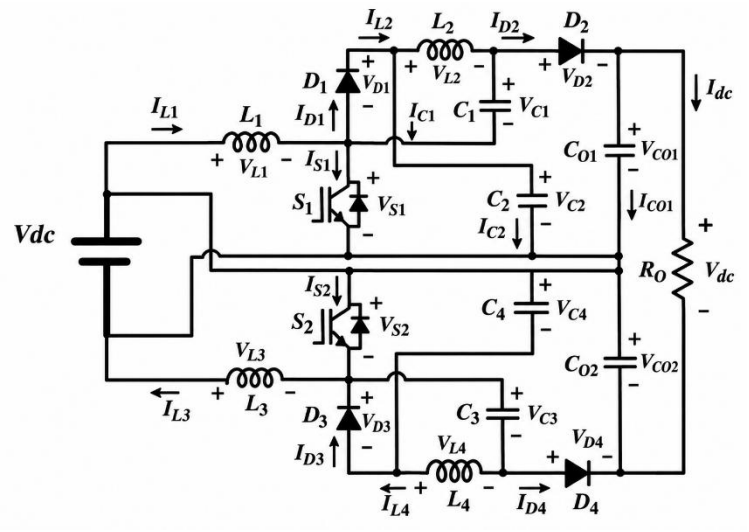

Figure 6. Model of interleaved KY converter

3.2. Interleaved KY converter

It is well known that the KY converter with the interleaved structure, namely the interleaved KY converter (IKYC), has high voltage gain and good power conversion efficiency. It achieves current ripple reduction and current stress distribution between the parallel phases through its interleaved operation. It may eliminate the voltage stress on semiconductors and reduce conduction and switching losses depending on circuit configuration and operating conditions. The IKYC is ideal for PV-integrated EV charging applications that demand high efficiency and stable voltage regulation.

Applications requiring operation under low-noise conditions use the Interleaved KY converters for the generation of improved transient load response. Moreover, the output current of KY converters is non-pulsating in nature, but the voltage gain requires further enhancement. In a converter design like this, the switching voltage is lower than the output voltage. It also generates output current with decreased output voltage ripple and no pulsation. To get a substantial voltage gain, two-step-up KY converters are interleaved. The following equation is used to compute the voltage gain:

$$M = \frac{1+3D}{1-D} \tag{2}$$

The finest parts are used to construct the interleaved KY converter. Switches S_2, S_1 ; inductors L_1, L_2, L_3 and L_4; capacitors C_1,C_2, $and\ C_3$; diodes D_1 ,D_2 ,D_3 and D_4 are all components of the proposed converter. Additionally, capacitors C_{o1} and C_{o2} are linked to the exterior side. Figure 6 depicts the electrical circuit model for the interleaved KY converter.

Two modes, continuous conduction mode (CCM) and discontinuous conduction mode (DCM) are considered when the proposed interleaved KY converter is operating. The energy transfer is continuous in CCM, and energy ripple is reduced because the current of the inductor will not go negative. During a part of the switching cycle, the inductor current is reduced to zero in DCM, which is usually during light-load operation. The operating mode depends on how heavy the load is, and the duty cycle, switching frequency, and the values of the inductances.

3.2.1. CCM

The interleaved KY converter presented in this paper is in continuous conduction mode (CCM), which is divided into two switching periods: Mode 1 and Mode 2. Energy transfer control and maintaining the desired output voltage occur during each mode as the switching states occur, charging and discharging the inductors and capacitors. The circuit configurations are shown in Figures 7(a) and 7(b), and the voltage and current waveforms in the respective circuits are shown in Figure 7(c).

i) Mode 1 $(t_0 - t_1)$: In this mode, switches S2 and S1 are switched ON and the diodes are turned OFF. Figure 7 (a) illustrates the current flow path for this mode. As the input voltage V_{pv} rises, the current flowing through inductors steadily grows. When there is a lag, charge is stored in the capacitors C_1 and C_2 it is supplied to the load via the capacitors C_3, C_4 and end output capacitors C_{o1} and C_{o2}.

$$V_{L1(mode1)} = V_{L3(mode1)} = V_{PV} \quad (3)$$

$$V_{L2(mode1)} = V_{C2} - V_{C1} \quad (4)$$

$$V_{L4(mode1)} = V_{C4} - V_{C3} \quad (5)$$

ii) Mode 2 $(t_1, -t_2)$: The switches s_1 and s_2 are both configured to be off during Mode 2. The diodes as shown in Figure 7(b) are shown in an active state with charge conduction. The gradual loss of energy held in the inductor leads to a linear reduction in current. As a result, the capacitors C_2 and C_4 are charged in this mode. The two output capacitors, as well as the load, are powered by the $C_1 \, and \, C_3$ capacitors. When the switches are switched ON, this mode is terminated. As a result, the voltage across the inductor in CCM Mode 2 is represented by (5) to (9).

$$V_{L1(mode2)} = V_{PV} - V_{C2} \quad (6)$$

$$V_{L2(mode2)} = -V_{C1} \quad (7)$$

$$V_{L3(mode2)} = V_{PV} - V_{C4} \quad (8)$$

$$V_{L4(mode2)} = -V_{C3} \quad (9)$$

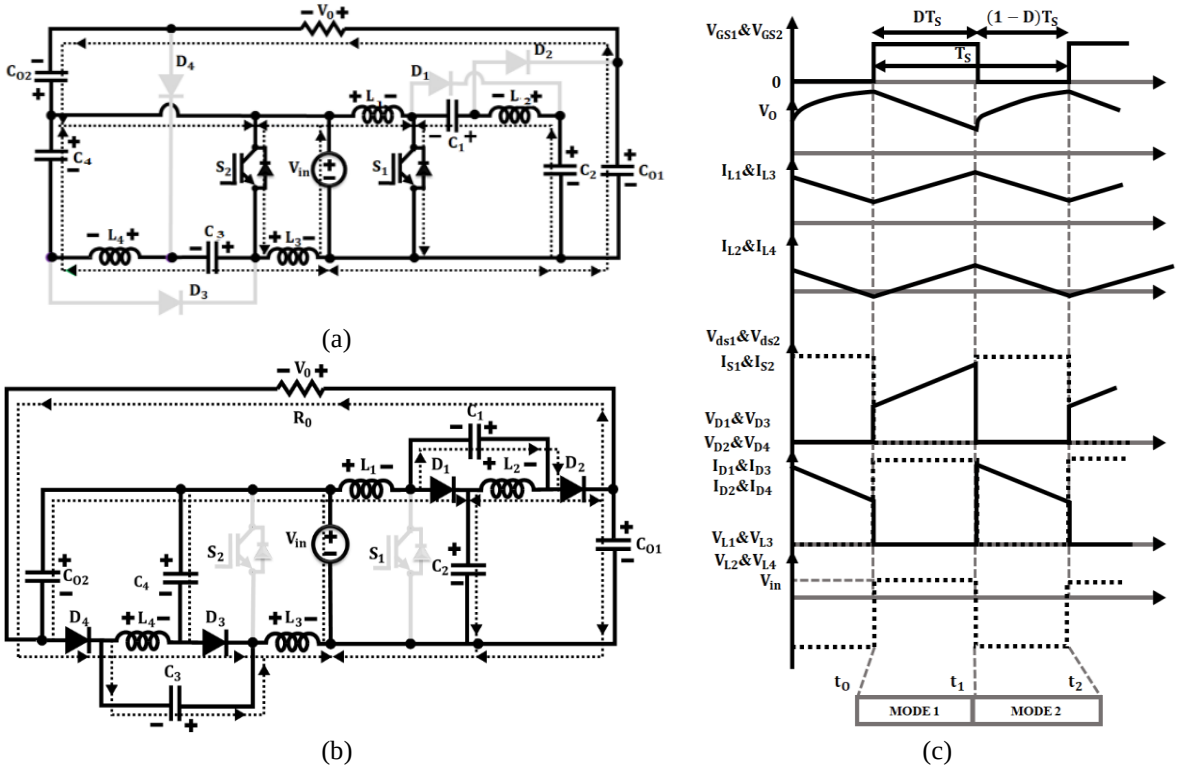

Figure 7. CCM Operation of IKYC in (a) Mode 1, (b) Mode 2, and (c) waveform

3.2.2. DCM

The circuit for IKYC in DCM mode 3 is presented in Figure 8(a), and the associated waveform is presented in Figure 8(b). Both DCM and CCM have the same initial working mode. Switches $S_1 and \, S_2$ and diodes $D_1, D_2, D_3, and \, D_4$ turn off when the diode current declines from Mode 2 to Mode 3 and approaches zero, and the outcome is that the inductor has no voltage.

(a)

(b)

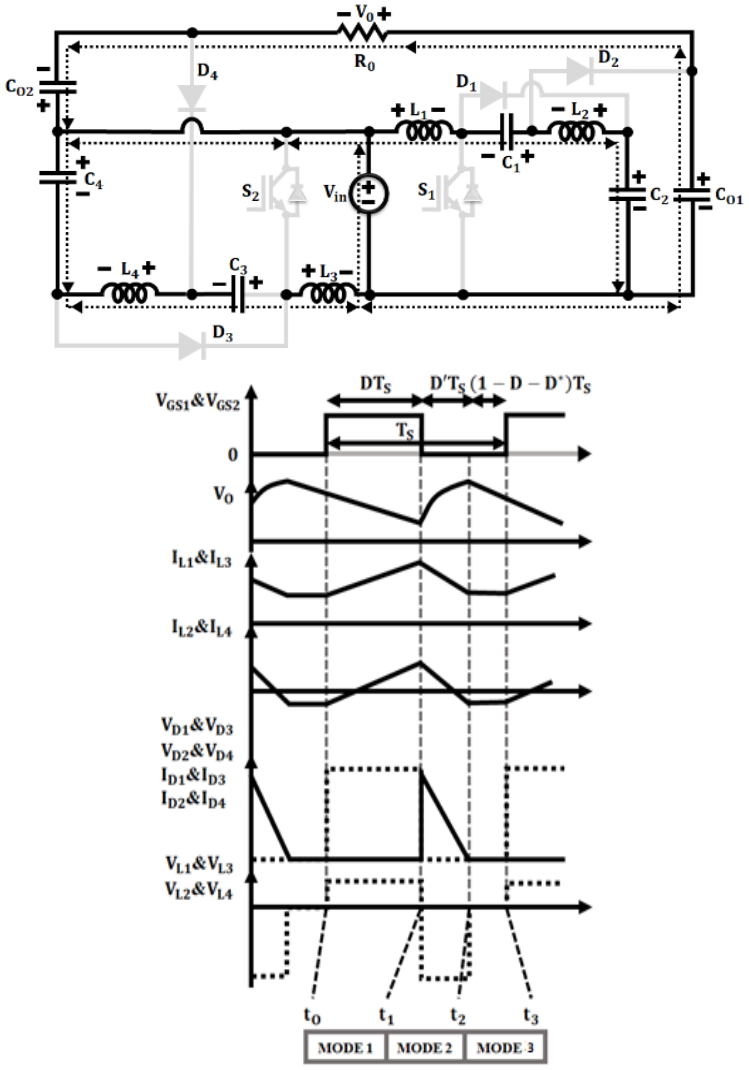

Figure 8. DCM operation of IKYC in (a) Mode 3 and (b) waveform

The performance of the converters in CCM mode is evaluated in the main mode using Kirchhoff's voltage law.

$$V_{dc} = V_{Co1} - V_{PV} + V_{Co2} \quad (10)$$

The expression's evaluation in the second operating mode is as in (11) and (12).

$$V_{Co1} = V_{C1} + V_{C2} \quad (11)$$

$$V_{Co2} = V_{C3} + V_{C4} \quad (12)$$

The (13)-(16) represents the voltage across capacitors $C_1, C_{2,}$ C_3, and C_4.

$$V_{C1} = \frac{D}{1-D} V_{PV} \quad (13)$$

$$V_{C2} = \frac{1}{1-D} V_{PV} \quad (14)$$

$$V_{C3} = \frac{D}{1-D} V_{PV} \quad (15)$$

$$V_{C4} = \frac{1}{1-D} V_{PV} \quad (16)$$

When the values of V_{C1} and V_{C2} are substituted into (11).

$$V_{Co1} = \frac{D+1}{1-D} V_{PV} \quad (17)$$

In (12), by considering V_{C3} and V_{C4}:

$$V_{Co2} = \frac{D+1}{1-D} V_{PV} \quad (18)$$

Therefore, the gain of an interleaved KY converter is determined as (19).

$$M_{CCM} = \frac{V_{dc}}{V_{PV}} = \frac{1+3D}{1-D} \quad (19)$$

This demonstrates the extremely high voltage conversion efficiency of the designed interleaved KY converter, which generates a controlled output at a DC link. Moreover, this DC voltage is applied to a vector-controlled topology for energizing the SR motor. The effective converter operation, along with the speed control approach, facilitates improved operation of the SR motor, which is corroborated by the results obtained as presented below:

3.3. Bi-directional converter

An efficient energy storage system is needed to tackle the intermittency of renewable energy sources. Typically, solar PV systems are connected to a battery and the grid to provide a continuous power supply [26]. A bidirectional DC–DC converter (BDC) can be used to allow bidirectional power flow between the battery and the DC bus, charging and discharging the battery and also increasing the stability and reliability of the system [27]. The basic configuration of the BDC is shown in Figure 9(a), which consists of two modes of operation: charging mode, when energy is fed from the DC grid to the battery, and discharging mode, when the stored battery energy is fed to the DC grid when PV energy is not available [28].

This session will demonstrate non-isolated bidirectional step up/down DC-DC converter design for battery charging and discharging. An inductor is the only energy storage device required for this system. It offers bidirectional power flow for battery charging and discharging by utilizing two bidirectional switches, such as MOSFETs or IGBTs. The benefits of this technique include fewer components, lower costs, less weight, and higher efficiency. Figure 9(b) depicts the bidirectional DC-DC converters that we employed in our study. The calculated values of various components of the BDC are given in Table 3.

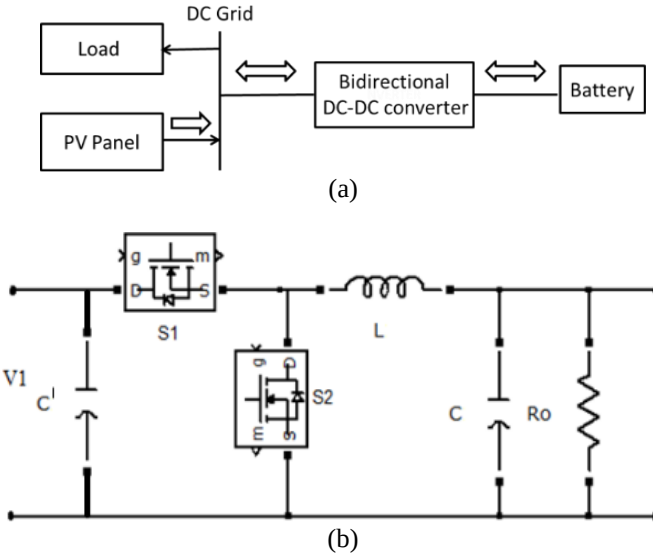

Figure 9. Configuration and circuit topology of the bidirectional DC–DC converter: (a) basic configuration and (b) converter circuit

Switch S1 is turned on for step-down mode, whereas switch S2 is turned on for step-up mode. The functioning of the converter is as follows:

i) Step-down mode

– Duty ratio: In (20) gives the duty ratio of the switch with a calculated efficiency of 90 to 95%.

$$D = \frac{V_{OUT}}{V_{IN}*\eta} = \frac{24}{48*0.9} = 0.55 \quad (20)$$

Where V_{IN} = input voltage, V_{OUT} = output voltage, and η = converter efficiency, e.g., estimated at 90 to 95%.

– Selection of inductor: The ripple current of the inductor is 10 to 20% of the output current. In (21) gives the ripple current of the inductor.

$$\Delta I_L = (0.1\ to\ 0.2) * I_{OUT}$$
$$\Delta I_L = 0.2\ A \quad (21)$$

Where I_{OUT} is the output current required by the application. Because of the reduced ripple in output current, the output current rises as the inductor value increases. The (22) is used to calculate the value of the inductor.

$$L = \frac{DTs*(V_d - V_o}{\Delta I_L})$$
$$L = 2.4\ mH \quad (22)$$

– Selection of output capacitor: The better practice is to utilise low ESR capacitors is to reduce output voltage ripple. In general, the ripple voltage is set to 10% of the output voltage. The values of output capacitors for an output voltage ripple are computed using (23).

$$C_{OUT} = \frac{(1-D)*V_{OUT}*TS^2}{8L*\Delta V_{OUT}}$$
$$C_{OUT} = 4.16\ \mu F \quad (23)$$

Where C_{OUT}= output capacitance, ΔV_{0UT} = output voltage ripple.

ii) Step-up mode:

– Duty ratio: The duty ratio of the switch with calculated efficiency of about 90 to 95% is given by (24).

$$D = 1 - \frac{V_{OUT}}{V_{IN}*\eta} = 0.55 \quad (24)$$

Where V_{IN} = input voltage, V_{OUT} = output voltage, and η = converter efficiency, e.g. estimated at 90 to 95%.

– Selection of inductor: The ripple current of the inductor is 10 to 20% of the output current. In (25) gives the ripple in inductor current.

$$\Delta I_L = (0.1\ to\ 0.2) * I_{IN}$$
$$\Delta I_L = 0.2\ A \quad (25)$$

Where I_{IN} is the input current required by the application. Because of the reduced ripple in output current, the output current rises as the inductor value increases. In (26) is used to calculate the value of the inductor.

$$L = \frac{DTs*(V_d}{\Delta I_L})$$
$$L = 2.4\ mH \quad (26)$$

– Selection of output capacitor: The better practice is to utilise low ESR capacitors is to reduce output voltage ripple. In general, the ripple voltage is set to 10% of the output voltage. The values of output capacitors for a desired output voltage ripple are computed using (27).

$$C_{OUT} = \frac{I_o * D}{f * \Delta V_o}$$

$$C_{OUT} = 41.6\ \mu F \quad (27)$$

Where C_{OUT} = output capacitance, ΔV_{0UT} = output voltage ripple.

The basic configuration of a bidirectional DC–DC converter for the DC grid, PV panel, load, and battery is shown in Figure 9(a). It allows power to be transferred both ways; thus, the battery may be charged by PV or grid power and may also provide power to the load when needed. The topology of the bidirectional DC–DC converter is shown in Figure 9(b), which includes two semiconductor switches (S1 and S2), an inductor (L), and capacitors on the input and output sides. The converter will transfer energy from the DC source to the battery during charging, and from the battery to the DC source during discharging. S1 and S2 switch on and off to control the direction of energy flow (power flow) and regulate the voltage, which helps in energy management in PV-integrated EV systems.

4. RESULTS AND DISCUSSION

Figure 10(a) depicts that the temperature is gradually maintained constant at 25 °C and it suddenly increases to 35˚ Celsius after 0.2 seconds, which is then remains constant. The solar irradiation is kept at 800 W/m² initially and is quickly switched to 1000 W/m² at 0.2 s, and then it is kept constant as detailed in Figure 10(b). In turn, the PV voltage is stabilized at about 130 V at the initial time and reaches 145 V at 0.2 s and remains there after this, as depicted in Figure 10(c). The PV current initially increases and then decreases to a value of about 2 A, as shown in Figure 10(d), and is then nearly constant. The output voltage, current, and inductor current waveforms of the SEPIC converter are shown in Figures 11(a) and 11(b).

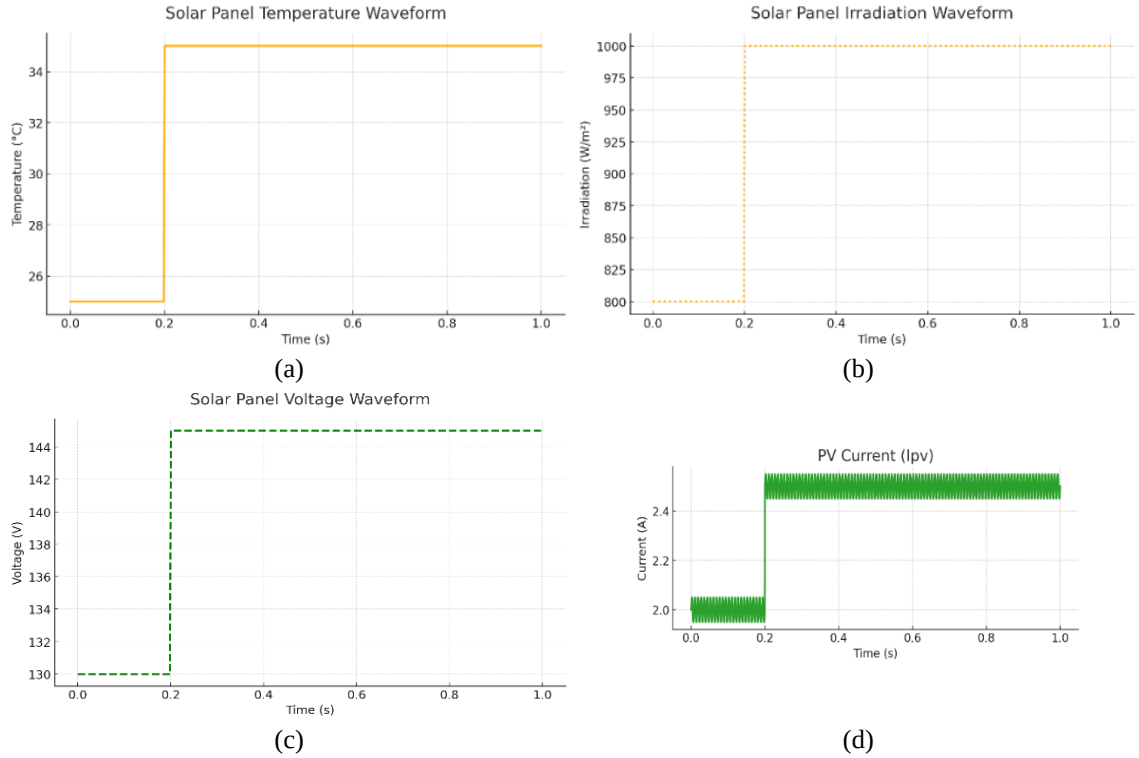

Figure 10. Response of the solar panel: (a) temperature, (b) irradiation, (c) voltage, and (d) current

The SEPIC converter is used to successfully raise the voltage of the solar panel from 145 V to ~ 170 v. The increased voltage is given to the inverter; the diagram is shown in Figure 11(a). The converter output current is found to be about 3 A, as shown in Figure 11(b), which shows that the converter can effectively boost the voltage and transfer the power. The SEPIC inductor current is shown in Figure 11(c).

The voltage and current responses of the conventional boost converter in the transient and steady-state operating conditions are shown in Figure 12(a) and 12(b), respectively. The output voltage also shows

an underdamped transient response, with initial oscillations followed by a steady output around 260 V. Also, the inrush current shows a transient due to switching operation and transient energy transfer through the inductor and capacitor. The current in the system tends to maintain the same operating value as a steady state is approached, and is approximately 18 A, which is consistent with the converter operating in a stable manner under these conditions. These responses show that the boost converter can deliver the desired output voltage and current; however, some oscillations are seen at the beginning when the converter is turned on to show that transient stress may exist during the start-up phase.

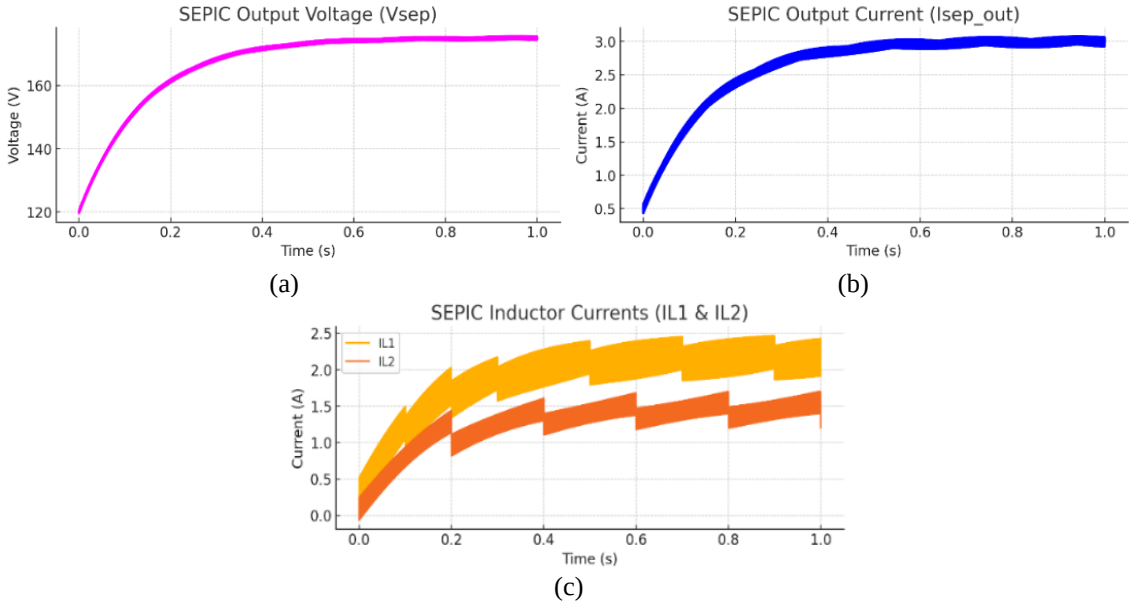

Figure 11. SEPIC converter response in (a) voltage, (b) current, and (c) inductor current

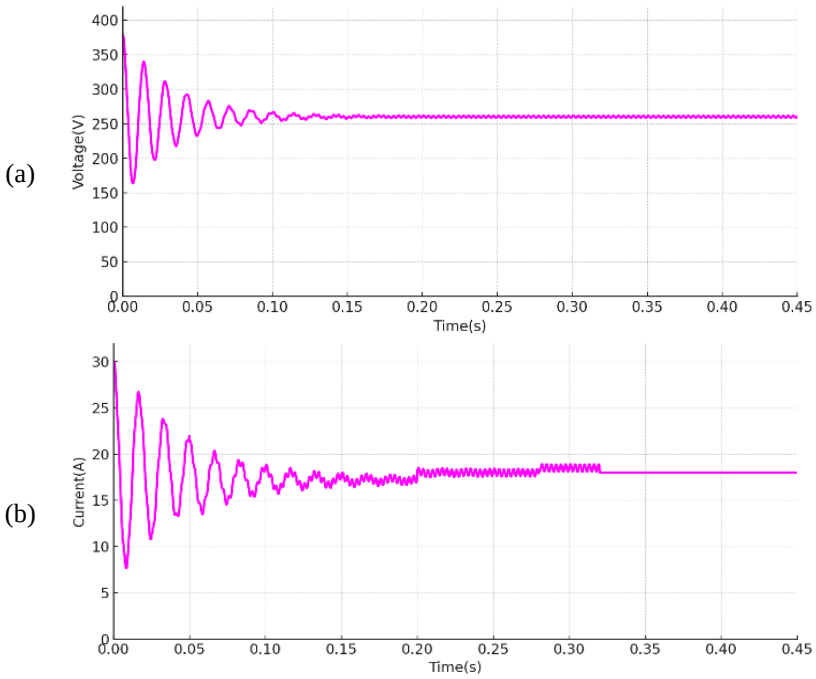

Figure 12. Boost converter response in (a) voltage and (b) current

The current and voltage responses of the interleaved boost converter are shown in Figures 13(a) and 13(b), respectively. Like the standard boost converter, the output voltage transiently oscillates before coming to rest around 260 V. Inrush current also changes during the initial transient period and then levels off at around 18 A when the steady-state condition is reached. Interleaved configuration, however, provides a way of dividing the input current between multiple parallel phases and applies phase-shifted switching signals to these phases, which can deliver a lower current ripple and spread electrical stress amongst the switching elements. It is therefore expected that this configuration would yield a smoother current characteristic as compared to a conventional boost converter working under similar operating conditions. To determine the level of improvement presented by the interleaved topology, a quantitative comparison is needed for the voltage overshoot, settling time, and current ripple.

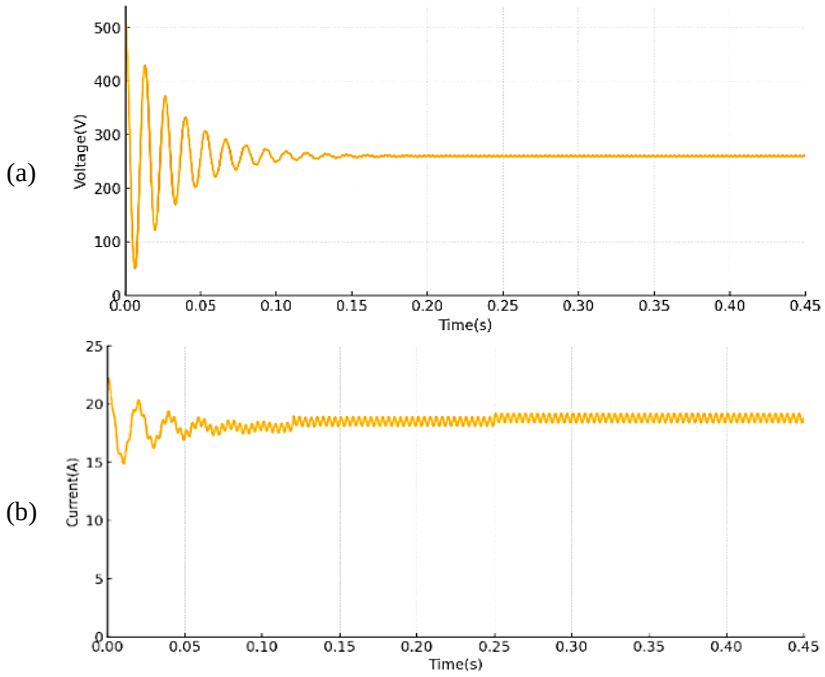

Figure 13. Interleaved boost converter response in (a) output voltage and (b) output current

Figures 14(a) and 14(b) present the current and voltage response of the interleaved KY converter, an underdamped transient with oscillations that gradually settle to a steady value around 260 V. The inrush current also oscillates initially and then stabilizes to a constant operating current near 18 A as the system reaches steady state. The waveform of the IKYC shows a fast-transient response with very low ripple compared to boost and interleaved boost converter (IBC) topologies. Due to the non-pulsating output current and phase-ripple cancellation, the IKYC achieves superior voltage stability and minimal oscillations.

Figure 15 illustrates the comparison of voltage for different DC-DC converters. The boost converter shows the largest overshoot and strongest oscillations, indicating a highly under-damped response and high output ripple during start-up. The IBC reduces both overshoot and oscillations because the two phase-shifted inductors share the load and partially cancel ripple. The interleaved KY converter (IKYC) exhibits the smoothest and most stable voltage response, with the smallest ripple and fastest settling due to its non-pulsating output current and effective ripple cancellation.

Figure 16 shows the comparison of output current for different DC-DC converters. The boost converter exhibits the highest inrush current, strongest oscillations, and the slowest damping due to its single-phase structure, which forces all ripple to flow through one inductor. The IBC reduces the peak current and ripple because the two interleaved inductors share the load and partially cancel each other's ripple components. The IKYC shows the smoothest and most stable current response, with very low oscillations and the fastest settling time, thanks to its non-pulsating output current characteristic and effective ripple cancellation across phases.

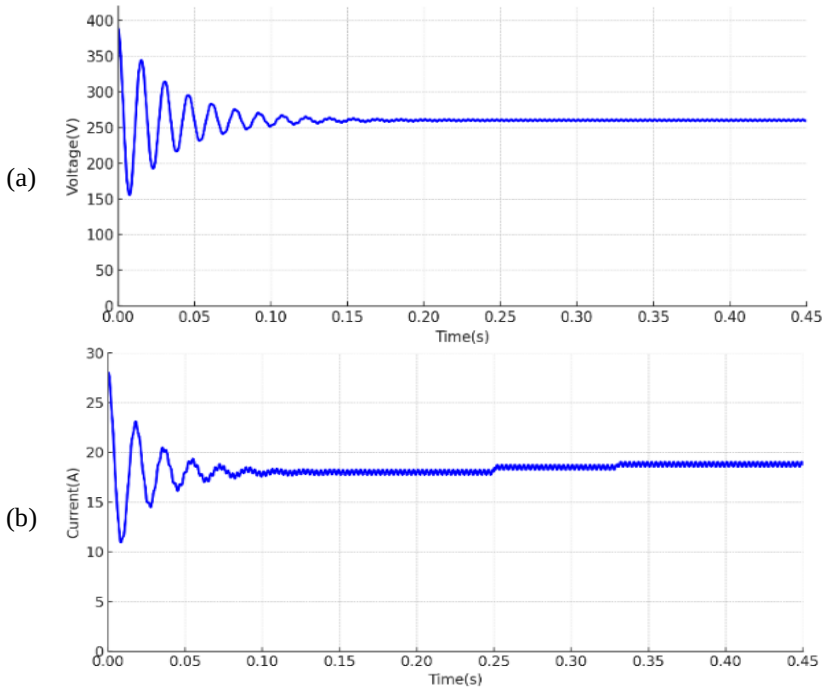

Figure 14. Interleaved KY converter: (a) output voltage and (b) output current

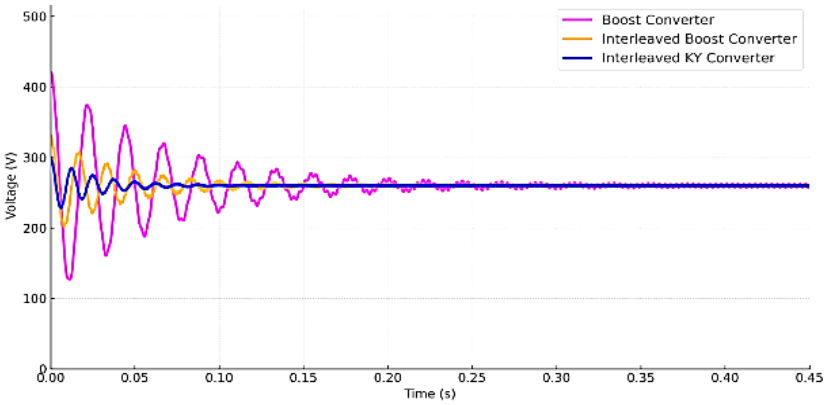

Figure 15. Comparison of output voltage for different DC–DC converters

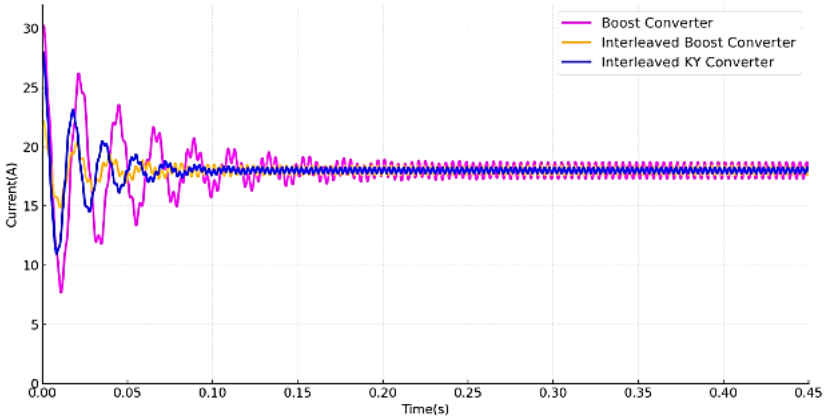

Figure 16. Comparison of output current for different DC–DC converters

5. COMPARATIVE ANALYSIS

5.1. Based on voltage gain

Many converters have been employed for EV converter. Figure 17 provides the comparison of different converters such as boost, IBC, and IKYC along with buck-boost, Cuk and KY converters with respect to the voltage gain. The buck-boost, Cuk, and KY converters are included for comparison because they are popular and more widely used power converters and comparing with them will give better understanding of enhanced voltage gain provided by IKYC. From the comparison, it is observed that IKYC possess higher voltage gain compared to other converters namely boost, buck-boost, cuk, IBC and IKYC whose voltage gains are in the ratio of 1:1.7, 1:2, 1:4 and 1:8 in given in Table 4.

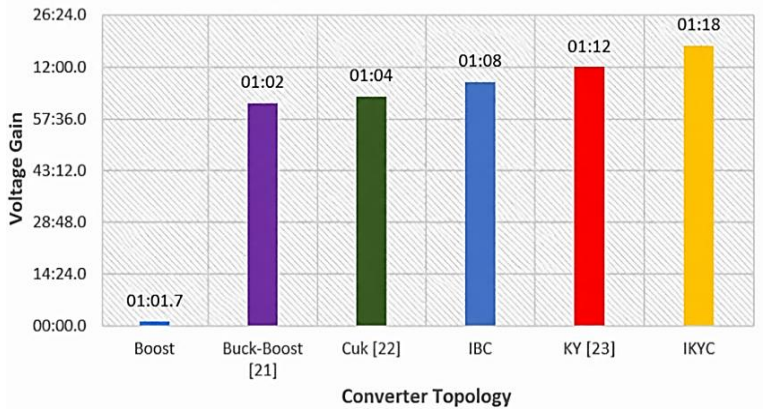

Figure 17. Voltage gain comparison of converters

5.2. Based on controller efficiency

The DC-DC converter boosts the EV converter output to the appropriate level; however, the DC-link voltage at the converter output is not maintained constant. In the proposed work, IKYC is utilized to improve the output and for keeping constant DC-link voltage at the converter output, CFLC based closed loop technique is employed. Furthermore, the performance of CFLC techniques is investigated by comparing it with controllers such as FLC and P&O, and the outcomes are tabulated in Table 5.

Figure 18 shows a comparative analysis of the proposed cascaded fuzzy logic controller (CFLC) with other controllers considered in this study, in which the proposed CFLC shows an efficiency of about 94%. The cascaded control structure of this improvement is responsible for its ability to provide the correct voltage and current control to achieve effective power conversion. As a result, the CFLC offers enhanced control performance in various operating points and load variations. The results show the feasibility of the proposed CFLC to improve the efficiency and dynamic performance of the interleaved KY converter in EV charging applications.

5.3. Based on converter efficiency

Efficiency is the main consideration that decides the significance of any system and converter. Moreover, the efficiency of the converter depends on voltage gain; that is, it increases with an increase in voltage gain. Here, to evaluate the importance of the proposed interleaved KY converter, it is compared with other existing converters, and the results are tabulated in Table 6, and the outcomes are pictorially represented in Figure 19. It is identified that the interleaved KY converter performs well with respect to efficiency, compared to other converters considered, and the efficiency is about 98% for IKYC, while other converters have an efficiency of 84.68%, 86%, 94%, and 95%.

5.4. Based on converter settling time

The settling time, which is the time taken by the output to respond to the changes in the step input, is considered to be one of the main parameters of the system efficiency. Hence, the time at which the output voltage of the IKYC settles down, maintaining a constant DC link voltage, is compared with the settling time attained by other converters considered for analysis. Table 7 presents the settling times of different converters. It can be inferred that the IKYC settles the output voltage much faster compared to other converters considered for analysis.

Table 4. Voltage gain comparison

Converters	Gain value	Converters	Gain value
Boost	1:1.7	IBC	1:8
Buck-boost [21]	1:2	KY [23]	1:12
Cuk [22]	1:4	IKYC	1:18

Table 5. Comparison for different controllers

Sl. No	Controllers	Efficiency
1.	P&O [19]	76%
2.	FLC [20]	87%
3.	CFLC	94%

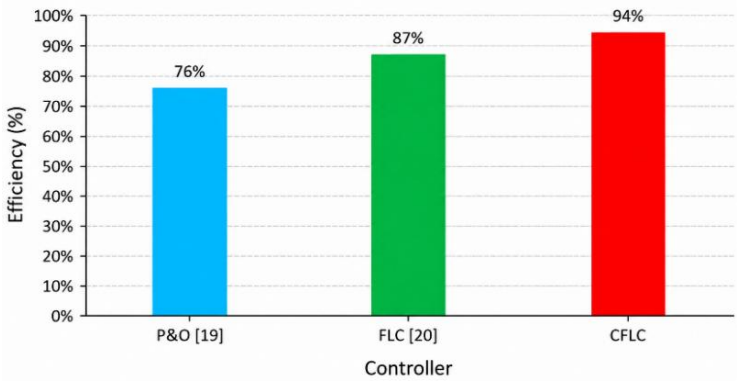

Figure 18. Comparison of different controllers efficiency

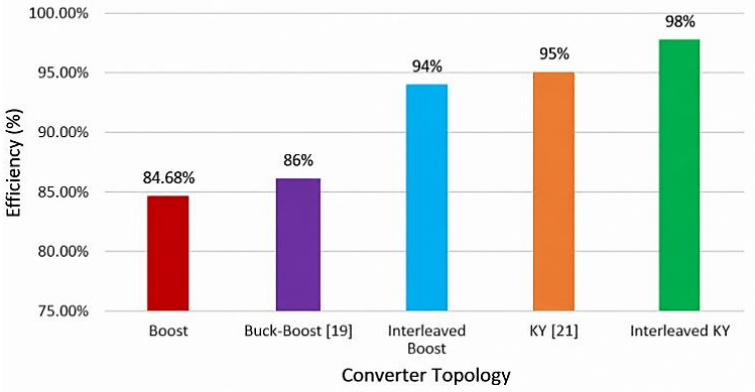

Figure 19. Efficiency comparison of converters

Table 6. Converter efficiency comparison

Sl. No	Converters	Efficiency	Sl. No	Converters	Efficiency
1.	Boost	84.68%	4.	KY [21]	95%
2.	Buck-boost [19]	86%	5.	Interleaved KY	98%
3.	Interleaved boost	94%			

Table 7. Settling time comparison

Controller	Converter		
	Boost	Interleaved boost	Interleaved KY
P&O control [19]	0.38s	0.31s	0.27s
Fuzzy control [20]	0.32s	0.26s	0.24s
CFCL	0.3s	0.28s	0.2s

6. CONCLUSION

The comparative evaluation of different converter topologies and control strategies clearly demonstrates that the proposed IKYC equipped with a CFLC delivers superior performance for PV-fed EV charging applications. According to the voltage-gain study, the IKYC attains the greatest gain of 1:16, better than boost (1:1.5), Cuk (1:3), buck-boost (1:2), KY (1:10), and interleaved boost (1:8) converters, showing its ability to boost the PV voltage to the required EV charging level. Further analysis of control methods reveals that the CFLC attains the greatest efficiency of about 94%, better than traditional FLC (87%) and P&O (76%). This confirms the recommended controller's ability to sustain a stable DC-link and improve dynamic control. In terms of converter efficiency, IKYC achieves the greatest efficiency of 98%, better than boost converters (84.68%), KY (95%), buck-boost (86%), and interleaved boost (94%). This shows that the combo of interleaved KY topology reduces the switching and conduction, leading to greater energy

conversion. In terms of settling-time study, it further demonstrates the dynamic benefits of the proposed system. The IKYC attains the quickest settling time of 0.20 s for CFLC control, whereas interleaved boost (0.28 s) and boost converters (0.30 s). The IKYC consistently achieves the quickest settling time of 0.27 s for P&O and 0.24 s for FLC, respectively, indicating superior transient efficiency and fast voltage stabilization. In conclusion, the analyses show that the proposed IKYC-based design offers the greatest voltage gain, better controller efficiency, higher converter efficiency, and the quickest dynamic response of all the systems tested. These findings indicate that the combination of IKYC with CFLC is a more reliable, energy-efficient, and high-performance choice for future PV-based EV charging and integration into the smart grid.

FUNDING INFORMATION

This research received no specific grant from any funding agency in the public, commercial, or not-for-profit sectors.

AUTHOR CONTRIBUTIONS STATEMENT

This journal uses the Contributor Roles Taxonomy (CRediT) to recognize individual author contributions, reduce authorship disputes, and facilitate collaboration.

Name of Author	C	M	So	Va	Fo	I	R	D	O	E	Vi	Su	P	Fu
M. Vaigundamoorthi	✓		✓		✓			✓	✓				✓	
G. Jegadeeswari	✓	✓	✓	✓	✓	✓		✓	✓	✓			✓	
S. Asha		✓				✓		✓	✓		✓	✓		
Savitha Venkatesan	✓		✓	✓			✓			✓	✓		✓	
R. Sundar	✓		✓		✓	✓		✓		✓			✓	
S. P. Manikandan	✓		✓	✓	✓			✓		✓			✓	
P. Veera Manikandan	✓		✓	✓	✓			✓		✓			✓	
Malathy Batumalay	✓	✓		✓	✓			✓	✓				✓	

C : **C**onceptualization
M : **M**ethodology
So : **So**ftware
Va : **Va**lidation
Fo : **Fo**rmal analysis
I : **I**nvestigation
R : **R**esources
D : **D**ata Curation
O : Writing - **O**riginal Draft
E : Writing - Review & **E**diting
Vi : **Vi**sualization
Su : **Su**pervision
P : **P**roject administration
Fu : **Fu**nding acquisition

CONFLICT OF INTEREST STATEMENT

The authors declare that they have no conflict of interest.

DATA AVAILABILITY

No new data were generated or analyzed in this study.

REFERENCES

[1] M. Yilmaz and P. T. Krein, "Review of charging power levels and infrastructure for plug-in electric and hybrid vehicles," in *2012 IEEE International Electric Vehicle Conference, IEVC 2012*, Mar. 2012, pp. 1–8, doi: 10.1109/IEVC.2012.6183208.

[2] M. A. Albadrani *et al.*, "Performance comparison of intelligent energy management strategies for hybrid electric vehicles with photovoltaic fuel cell and battery integration," *Batteries*, vol. 12, no. 4, 2026, doi: 10.3390/batteries12040147.

[3] G. Ramkumar, S. Kannan, V. Mohanavel, S. Karthikeyan, and A. Titus, "The future of green mobility: a review exploring renewable energy systems integration in electric vehicles," *Results in Engineering*, vol. 27, 2025, doi: 10.1016/j.rineng.2025.105647.

[4] A. Kochanek *et al.*, "Renewable energy integration in sustainable transport: a review of emerging propulsion technologies and energy transition mechanisms," *Energies*, vol. 18, no. 24, 2025, doi: 10.3390/en18246610.

[5] S. Joni, A. Bhattacharya, and S. Das, "A novel modified interleaved high-gain DC-DC converter using asymmetrical voltage multiplier and coupled inductor with leakage energy recycling," in *3rd International Conference on Power Electronics and Energy, ICPEE 2025*, Bhubaneswar, India, 2025, pp. 1–6, doi: 10.1109/ICPEE65973.2025.11410901.

[6] R. Brindha and S. Rathinamala, "Modeling and control of SEPIC converters in hybrid microgrid application using exact linearization technique," in *International Conference on Advancements in Power, Communication and Intelligent Systems, APCI 2024*, Kannur, India, 2024, pp. 1–6, doi: 10.1109/APCI61480.2024.10617425.

[7] T. Muthamizhan, C. Rithika, S. Avanthika, and M. Sriranjanichellam, "A high gain SEPIC DC/DC converter for renewable energy applications," in *2025 6th International Conference for Emerging Technology, INCET 2025*, May 2025, pp. 1–6, doi: 10.1109/INCET64471.2025.11139931.

[8] Asif, W. Ahmad, M. B. Qureshi, M. M. Khan, M. A. B. Fayyaz, and R. Nawaz, "Optimizing large-scale PV systems with machine learning: a neuro-fuzzy MPPT control for PSCs with uncertainties," *Electronics (Switzerland)*, vol. 12, no. 7, 2023, doi: 10.3390/electronics12071720.
[9] A. El Khateb, N. A. Rahim, J. Selvaraj, and M. N. Uddin, "Fuzzy-logic-controller-based SEPIC converter for maximum power point tracking," *IEEE Transactions on Industry Applications*, vol. 50, no. 4, pp. 2349–2358, 2014, doi: 10.1109/TIA.2014.2298558.
[10] J. Cao and A. Emadi, "A new battery/ultracapacitor hybrid energy storage system for electric, hybrid, and plug-in hybrid electric vehicles," *IEEE Transactions on Power Electronics*, vol. 27, no. 1, pp. 122–132, 2012, doi: 10.1109/TPEL.2011.2151206.
[11] F. Ibanez, "Hybrid energy storage systems in electric vehicle applications," *Electric Vehicles - Design, Modelling and Simulation*. Sep. 2023, doi: 10.5772/intechopen.113000.
[12] H. Yu, C. Wu, and Y. Liu, "Vehicle-to-grid integration in smart energy systems: an overview of enabling technologies, system-level impacts, and open issues," *Machines*, vol. 14, no. 4, 2026, doi: 10.3390/machines14040418.
[13] F. A. Silva, "Modern electric, hybrid electric, and fuel cell vehicles, third edition [book news]," *IEEE Industrial Electronics Magazine*, vol. 12, no. 4, pp. 46–48, Dec. 2018, doi: 10.1109/mie.2018.2874371.
[14] M. Kavitha and V. Sivachidambaranathan, "High-voltage gain DC–DC converter for renewable energy applications," in *Advances in Intelligent Systems and Computing*, vol. 1040, 2020, pp. 657–669, doi: 10.1007/978-981-15-1451-7_67.
[15] A. A. Shalbaf, N. Shahidi, and M. Hemati, "A high-gain interleaved DC-DC converter with reduced components for EV charging application," *Computers and Electrical Engineering*, vol. 118, May 2024, doi: 10.1016/j.compeleceng.2024.109316.
[16] D. Sathya, G. Saravanan, and R. Thangamani, "Fuzzy logic and its applications in mechatronic control systems," in *Computational Intelligent Techniques in Mechatronics*, Wiley, 2024, pp. 211–241, doi: 10.1002/9781394175437.ch7.
[17] W. C. So, C. K. Tse, and Y. S. Lee, "Development of a fuzzy logic controller for DC/DC converters: design, computer simulation, and experimental evaluation," *IEEE Transactions on Power Electronics*, vol. 11, no. 1, pp. 24–32, 1996, doi: 10.1109/63.484413.
[18] B. Kirubadurai, R. Jaganraj, M. Vinothkumar, and G. Jegadeeswari, "A dual modelling approach: CFD and electrochemical impedance spectroscopy for enhanced PEM fuel cell design and operation," *Results in Engineering*, vol. 26, Jun. 2025, doi: 10.1016/j.rineng.2025.104858.
[19] N. H. Baharudin, T. M. N. T. Mansur, F. A. Hamid, R. Ali, and M. I. Misrun, "Topologies of DC-DC converter in solar PV applications," *Indonesian Journal of Electrical Engineering and Computer Science*, vol. 8, no. 2, pp. 368–374, Nov. 2017, doi: 10.11591/ijeecs.v8.i2.pp368-374.
[20] Y. Fang *et al.*, "A 98.0% Efficiency GaN-based intermediate bus converter (IBC) with bidirectional full-wave current sensor and near-zero dead-time GaN driver for data center applications," in *2026 IEEE Applied Power Electronics Conference and Exposition (APEC)*, IEEE, Mar. 2026, pp. 1684–1687, doi: 10.1109/APEC51134.2026.11516679.
[21] S. Mandal and P. Prabhakaran, "A high-efficiency, high-gain, non-isolated bidirectional DC-DC converter for interfacing dc grid-connected energy storage systems," *IEEE Transactions on Consumer Electronics*, vol. 72, no. 1, pp. 134–146, Feb. 2026, doi: 10.1109/TCE.2025.3648303.
[22] S. Savio, S. Giuffrida, F. Mandrile, F. Stella, E. G. Armando, and R. Bojoi, "Digital control of multilevel interleaved GAN DC-DC converter for fuel cell electric powertrains," *IEEE Transactions on Industry Applications*, vol. 62, no. 2, pp. 2723–2734, Mar. 2026, doi: 10.1109/TIA.2025.3599817.
[23] I. Etier, K. Balachander, G. Kavitha, G. Sureshkumaar, and N. Kannan, "Design and performance assessment of SEPIC converter for the grid-connected PV system," in *3rd International Conference on Smart Electronics and Communication, ICOSEC 2022 - Proceedings*, Trichy, India, 2022, pp. 235–244, doi: 10.1109/ICOSEC54921.2022.9951911.
[24] S. Ramya *et al.*, "Smart solid waste collection for a sustainable smart city using Arduino Uno," in *2023 International Conference on Computer Communication and Informatics, ICCCI 2023*, Jan. 2023, pp. 1–5, doi: 10.1109/ICCCI56745.2023.10128183.
[25] B. A. Vijayalakshmi, C. J. De Britto, V. J. Ramya, and R. S. Devi, "Smart city lighting with solar-powered VLC-enabled LEDs using AOD-OFDM for sustainable communication and illumination," *Journal of Optics (India)*, Feb. 2025, doi: 10.1007/s12596-025-02632-8.
[26] S. Vazquez, S. M. Lukic, E. Galvan, L. G. Franquelo, and J. M. Carrasco, "Energy storage systems for transport and grid applications," *IEEE Transactions on Industrial Electronics*, vol. 57, no. 12, pp. 3881–3895, 2010, doi: 10.1109/TIE.2010.2076414.
[27] M. Owais Khan, S. Kirmani, and M. Rihan, "Impact assessment of electric vehicle charging on distribution networks," *Renewable Energy Focus*, vol. 50, 2024, doi: 10.1016/j.ref.2024.100599.
[28] S. M. Ho, M. A. Mahadik, J. S. Jang, and V. N. Singh, "Metal oxide-based chalcogenide heterostructure thin film photoanodes for photoelectrochemical solar hydrogen generation," *Asian Journal of Chemistry*, vol. 31, no. 1, pp. 18–24, 2019, doi: 10.14233/ajchem.2019.21647.

BIOGRAPHIES OF AUTHORS



Dr. M. Vaigundamoorthi is a faculty member in the Department of Electrical and Electronics Engineering at Saveetha Engineering College, Chennai 602105, India. He received his B.E. degree in electrical and electronics engineering from Madurai Kamaraj University in 2002. He obtained his Master of Engineering degree in power electronics and drives and his Ph.D. degree in power electronics, specializing in DC–DC converters for solar photovoltaic (PV) systems, from the College of Engineering, Guindy (CEG), Anna University, Chennai, India, in 2007 and 2013, respectively. He has 22 years of teaching experience and has published 15 research articles in reputed international journals and holds six patents. His research interests include power electronics for renewable energy systems, controller design, and nonlinear dynamics analysis in solar PV systems. He can be contacted at email: vaigundamoorthim@saveetha.ac.in.



Dr. G. Jegadeeswari is an assistant professor in the Department of Electrical and Electronics Engineering at Saveetha Engineering College (Autonomous), Chennai, where she has been serving since 2024. She received her B.Tech. degree in electrical and electronics engineering and her M.Tech. degree in power electronics and drives from Pondicherry University in 2007 and 2012, respectively. She obtained her Ph.D. degree from the Faculty of Electrical and Electronics Engineering at AMET University, Chennai, in 2024. With over 13 years of teaching experience and six years of research experience, she has published more than 100 research articles, 30 of which are indexed in Scopus. She is a member of professional organizations, including IEEE and ISOR, and holds three national and international patents. She has also authored three textbooks, edited one book, and contributed eight book chapters published by renowned publishers, including IGI Global, CRC Press, Bentham Science, and Wiley. In addition, she has organized more than 70 workshops, faculty development programs (FDPs), seminars, and conferences at the departmental and university levels. She has submitted research proposals to several funding agencies and organizations, including TNSCST, AICTE, DST, NCW, and SERB, and secured an ATAL FDP grant of INR 270,000. Her academic contributions have earned her several accolades, including Best Teacher and Best Paper awards from various institutions. She also serves as a reviewer and editorial board member for several international journals. Her research interests include power electronics and drives, special machines, and renewable energy. She can be contacted at email: jegadeeswari.dharan@gmail.com.



Dr. S. Asha received her B.E. degree in electronics and communication engineering from Madras University and her M.Tech. degree in applied electronics from Dr. M.G.R. Research Institute. She conducted her doctoral research in very-large-scale integration (VLSI) and obtained her Ph.D. degree from St. Peter's Research Institute. She is currently a professor at Saveetha Engineering College, Chennai, India. She has 25 years of experience in both industry and academia and has published several research papers in national and international journals and conference proceedings. Her research interests include antennas and microwave engineering. She is a Fellow of IETE. She can be contacted at email: asha@saveetha.ac.in.



Dr. Savitha Venkatesan received her B.E. degree in electrical and electronics engineering from Madras University, India, in 2003, her M.E. degree in power systems engineering from Anna University, India, in 2007, and her Ph.D. degree in power systems engineering from Anna University, India, in 2025. She is currently an assistant professor in the Department of Electrical and Electronics Engineering at Saveetha Engineering College, Chennai, India. She has over 16 years of teaching experience and has published 10 research works in national and international journals, conference proceedings, and book chapters. She holds two published patents and two granted patents. Her research interests include power electronic converters, renewable energy systems, the Internet of Things (IoT), control systems, and microgrids. She is a member of the Institution of Engineers (India) and the Indian Society for Technical Education. She can be contacted at email: savinalan25@gmail.com.



Dr. R. Sundar is currently an associate professor of marine engineering at AMET Deemed to be University, India. He received his Ph.D. degree in engineering and technology, specializing in renewable energy, from AMET University. He obtained his master's degree in power electronics and drives from Sri Padmavathi Institute of Higher Education and Research (SPIHER), affiliated with the Madras Institute of Technology (MIT) Campus, Anna University. He received his bachelor's degree in electrical and electronics engineering from the University of Madras. He has 22 years of teaching experience, with expertise in marine automation and control systems, marine electrical technology, electrical machines, renewable energy systems, the Internet of Things (IoT), and power electronics. He has published more than 25 research papers in reputed journals, including Scopus-indexed and Science Citation Index (SCI)-indexed journals, and has presented 35 papers at various international conferences. He is also the author of a textbook on the design of electrical machines, control systems, and electric and hybrid vehicles. He is a life member of the Institute of Research Engineers and Doctors (IRED) and the International Association of Engineers (IAENG). He has served as a member of the Academic Council and the Internal Quality Assurance Cell (IQAC) Core Team, president of the National Digital Library of India (NDLI) Club, coordinator of the Marine Technology Society (MTS) Student Chapter, and member of several committees, including the Library Committee. He can be contacted at email: mrsundarkrishna@gmail.com.



Dr. S. P. Manikandan holds a B.E. degree in electronics and communication engineering from PSN College of Engineering and Technology, affiliated with Anna University. He subsequently obtained his M.E. degree in embedded systems and technologies from Sri Ram Engineering College, also affiliated with Anna University. He completed his Ph.D. at Dr. M.G.R. Educational and Research Institute. He is currently working at Saveetha Engineering College, Thandalam, Chennai, India. His areas of specialization include digital electronics, circuits and devices, and linear integrated circuits. With over 15 years of teaching experience, he has continued to enhance his academic knowledge through participation in various NPTEL and SWAYAM courses. He has contributed to research and innovation through patent publications and book authorship. He has also presented papers at numerous national and international conferences and published research articles in reputed Scopus-indexed journals. He can be contacted at email: drmanikandansp@gmail.com.



Dr. P. Veera Manikandan received his B.E. degree in electrical and electronics engineering and his M.E. degree in power electronics and drives from Anna University, Chennai, in 2010 and 2012, respectively. He obtained his Ph.D. degree in electrical engineering from Anna University, Chennai, in 2021. He has published more than 25 research papers in national and international journals and conference proceedings and has 13 years of teaching experience. He is currently an associate professor in the Department of Electrical and Electronics Engineering at Dhanalakshmi Srinivasan College of Engineering and Technology, Mahabalipuram, Chennai, Tamil Nadu, India. His research interests include power electronics, solar maximum power point tracking (MPPT), multilevel inverters, and soft computing techniques. He can be contacted at email: veerarmd@gmail.com.



Dr. Malathy Batumalay earned her master's degree in engineering from the University of Malaya, Malaysia, and subsequently obtained her Ph.D. in photonics engineering from the same institution. Her research interests include lasers, fiber optics, and fiber-optic sensors. She has developed fiber-optic sensors capable of detecting changes in relative humidity and chemical solutions. She collaborates with local and international researchers to investigate the behavior and characteristics of fiber-optic and plasmonic sensors, resulting in numerous high-quality publications in relevant journals. She also serves as a reviewer for several journals and holds a committee position in the Optical Society of Malaysia (OSM), where she contributes to activities involving young researchers. Furthermore, she is registered as a professional engineer with the Board of Engineers Malaysia (BEM) and as a Chartered Engineer with the Institution of Engineering and Technology (IET). She is currently affiliated with a private university in Malaysia specializing in communication, networking, and cloud computing, where she holds several key leadership positions. She serves as the Director of the Center for Data Science and Sustainable Technologies, Chair of the University Research Committee, and Chief Internal Auditor for the Malaysia Research Assessment. She also serves as the Managing Editor of the Journal of Innovation and Technology (JOIT). She is passionate about engaging with emerging talents and prospective research candidates to contribute to the advancement of the academic community. She can be contacted at email: malathy.batumalay@newinti.edu.my.